*Canadian Mineralogist*
Vol. 28, pp. 859-874 (1990)

# EXPERIMENTAL AND THEORETICAL CONSTRAINTS ON ALUMINUM SUBSTITUTION IN MAGNESIAN CHLORITE, AND A THERMODYNAMIC MODEL FOR $H_2O$ IN MAGNESIAN CORDIERITE

DERRY C. McPHAIL[1], ROBERT G. BERMAN[2] AND HUGH J. GREENWOOD
*Department of Geological Sciences, University of British Columbia, Vancouver, British Columbia V6T 2B4*

## ABSTRACT

The equilibrium chlorite = cordierite + forsterite + spinel + $H_2O$ has been determined experimentally using a chlorite of composition $Mg_{4.75}Al_{2.5}Si_{2.75}O_{10}(OH)_8$. The results are in agreement with existing experimental data on the same reaction, where a chlorite of clinochlore composition [$Mg_5Al_2Si_3O_{10}(OH)_8$] was used. A thermodynamic analysis of the results includes a model describing the $H_2O$ content of magnesian cordierite. The experimental data from this and other related studies have been used to constrain the solution properties of aluminum exchange in magnesian chlorite. The results of the thermodynamic modeling have been used to identify mineral assemblages in which the composition of chlorite should be useful as a petrogenetic indicator. Comparison between predicted composition and measured composition of natural chlorite shows good agreement for most bulk compositions. Chlorite is predicted to become more aluminous with increasing temperature and decreasing pressure in assemblages found in metamorphosed ultramafic rocks (chlorite – forsterite – talc or orthopyroxene) and pelitic rocks metamorphosed at whiteschist-facies conditions (chlorite – talc – quartz). In contrast, chlorite in metamorphosed corundum-bearing rocks is predicted to become less aluminous with increasing temperature and decreasing pressure.

*Keywords*: experimental, thermodynamic, equilibrium, chlorite, cordierite, aluminum, solution model.

## SOMMAIRE

Nous avons déterminé la position de l'équilibre chlorite = cordiérite + forstérite + spinelle + $H_2O$ expérimentalement en utilisant une chlorite de composition $Mg_{4.75}Al_{2.5}Si_{2.75}O_{10}(OH)_8$. Les résultats concordent avec les données expérimentales disponibles pour le même équilibre impliquant la clinochlore, $Mg_5Al_2Si_3O_{10}(OH)_8$. L'analyse thermodynamique des résultats implique l'élaboration d'un modèle pour décrire la teneur en eau de la cordiérite magnésienne. Nos données expérimentales et celles d'autres études pertinentes ont servi à bien définir les échanges impliquant l'aluminium dans la solution solide qu'est la chlorite magnésienne. Le modèle thermodynamique peut servir à identifier les assemblages de minéraux dans lesquels la composition de la chlorite pourrait être un indicateur pétrogénétique; une comparaison entre composition prédite et composition mesurée de la chlorite naturelle montre une corcordance pour la plupart des compositions globales. La chlorite deviendrait de plus en plus alumineuse à mesure qu'augmente la température et que diminue la pression dans les assemblages des roches ultramafiques métamorphisées (chlorite – forstérite – talc ou orthopyroxène) et des roches pélitiques recristallisées dans le facies des schistes blancs (chlorite – talc – quartz). Par contre, dans les assemblages métamorphiques à corindon, la chlorite deviendrait de plus en plus alumineuse avec une augmentation en température et une diminution en pression.

(Traduit par la Rédaction)

*Mots-clés*: expérimental, thermodynamique, équilibre, chlorite, cordiérite.

## INTRODUCTION

Chlorite is present in rocks from many different geological environments, which is a reflection of its stability over a wide range in pressure, temperature and bulk composition. There is great potential for using the composition of chlorite to help understand the metamorphic history of rocks; however, this potential cannot be realized without quantitative knowledge of the thermodynamic properties of this complex solid-solution. Experimental phase-equilibrium studies provide constraints on such properties. There have been many studies published that deal with the stability of chlorite; see Chernosky *et al.* (1988) for a complete review. One of the important exchanges that occurs in chlorite is the magnesium-Tschermaks exchange, wherein the aluminum content of chlorite is sensitive to changes in pressure, temperature and mineral assemblage. This is perhaps most evident for magnesian chlorite, which occurs in metamorphosed ultramafic rocks, dolomites, high-pressure metapelitic rocks and high-aluminum, corundum-bearing metamorphic rocks. Experimental data have been published recently that provide information for the aluminum exchange in magnesian chlorite (Jenkins & Chernosky 1986); however, additional experimental data are required.

Several solution models for chlorite have been proposed in recent years (Walshe 1986, Stoessell 1984,

[1]Present address: Department of Geological and Geophysical Sciences, Princeton University, Princeton, New Jersey 08544, U.S.A.
[2]Present address: Geological Survey of Canada, 601 Booth Street, Ottawa, Ontario K1A 0E8.

Walshe & Solomon 1981), but all suffer from a lack of data for calibration. Walshe (1986) built upon the preliminary model of Walshe & Solomon (1981), based on six components to describe the composition of chlorite, assuming ideal mixing for all but one of the end-members; they calibrated their model using the composition of natural chlorite from different environments and locations. Stoessell (1984) used six end-members in a five-component reciprocal solution and assumed regular site-mixing for chlorite at 25°C. To calibrate his model, he used the solubility data of Kittrick (1982) and the standard-state properties of clinochlore derived by Helgeson *et al.* (1978). He calculated four sets of chemical potentials for his chosen end-members, based on different sets of exchange energies, but was not able to select a preferred set.

The purpose of this study was to provide additional constraints on the aluminum exchange in chlorite by measuring the high-temperature breakdown of magnesian chlorite to cordierite, forsterite, spinel and $H_2O$ using a chlorite more aluminous than clinochlore. This equilibrium was considered appropriate because 1) it has been previously reversed with a chlorite of clinochlore composition, and 2) the properties of clinochlore as well as those of the other phases involved are constrained from other phase-equilibrium, calorimetric and crystal-chemical studies.

## Experimental Method and Results

### *Starting materials*

An oxide mix was prepared from reagent-grade chemicals in the molar proportions $4.75MgO : 1.25Al_2O_3 : 2.75SiO_2$. Periclase was prepared by heating MgO (Fisher Certified Reagent, Lot #741694) for approximately 24 hours at 1300°C, and cristobalite, by baking silicic acid (Fisher Certified Reagent, Lot #730944) for approximately 24 hours at 1300°C. $Al_2O_3$ was prepared by heating $Al(OH)_3 \cdot nH_2O$ (Fisher Certified Reagent, Lot #745229) at 400°C for four hours, 700°C for one hour and 1000°C for one hour; X-ray powder diffraction showed $\alpha$-$Al_2O_3$ with no trace of corundum. The oxides were ground under alcohol and dried in a vacuum furnace for approximately 24 hours at 120°C before use. Appropriate proportions were carefully weighed out, and the mixture was ground for approximately two hours under distilled water in an agate mortar. To ensure homogeneity, the mixture was dried periodically and collected into the bottom of the mortar. The resulting mixture was then dried and stored in a desiccator.

Chlorite was synthesized from the oxide mix plus approximately 25 wt.% distilled water in two steps, 4 kbars, 400°C, 7 to 10 days and 4 kbars, 700°C, 14 to 18 days. The first step helped prevent extraneous phases such as spinel and forsterite from nucleating, and the second produced the stable 14 Å IIb polytype. An X-ray peak at about 19° 2$\theta$ (Cu$K\alpha$ radiation) indicated that there may have been a small amount of a 7 Å phase, formed during the low-temperature step and persisting metastably through the high-temperature step. A trace of spinel was identified optically, but it was not considered to significantly affect the composition of the chlorite. The amount of spinel was estimated to be less than 0.1% by volume from the Comparison Charts for Visual Estimation of Percentage Composition (Terry & Chilingar 1955); using volumes of spinel and chlorite of 40 and 210 $cm^3$, the change in the chlorite composition was calculated to be less than 0.01 atoms of aluminum per formula unit.

The high-temperature assemblage (cordierite, forsterite and spinel) was synthesized at 2 kbars and 740°C for 14 days from the run products of earlier, less successful syntheses of chlorite. No extraneous phases were detected by either X-ray diffraction or optical microscopy.

### *Experimental technique*

All experiments were conducted in horizontally mounted standard cold-seal pressure vessels of either Stellite K–25 or René 41 alloys, with a thermocouple mounted in an external thermocouple well. Each unit was calibrated at temperatures between 300 and 800°C (1 atmosphere). Temperature gradients were found to be less than $\pm 1$°C over the 3-cm length of the sample position. Temperatures were controlled to within $\pm 1$°C using fully proportional controllers, and precise daily measurements were made using either a temperature-compensated digital thermometer with a resolution of 1°C or a potentiometer with an estimated resolution of 0.1°C. Temperatures were not monitored continuously, but measurements were taken at different times of day to avoid possible systematic differences. None were noted. Quoted temperatures are the means of the daily measurements (corrected by the calibration determinations); the associated errors were determined by adding two standard deviations of the daily measurements, gradient uncertainties and an estimated 3°C for uncertainty in thermocouple calibration.

The pressure medium was either methane or distilled $H_2O$. Measurements were made every one to three days, usually daily, with either an Ashcroft Maxisafe gauge, with a resolution of 15 bars, or a Heise Bourdon tube gauge with a resolution of 5 bars. All gauges were checked periodically against a factory-calibrated Heise gauge to ensure accuracy. Experiments with pressure drops of more than 3% were discarded. The quoted pressures are the means of the measurements, and the associated errors are

sums of two standard deviations plus an estimated 20 bars for gauge accuracy.

The starting materials for most of the reversal experiments were made of two mixtures of reactants and products: 15–20 wt.% of the reactants plus 80–85 wt.% of the products, and 80–85 wt.% of the reactants plus 15–20 wt.% of the products. For some of the experiments, the starting materials consisted of either 100% chlorite or 100% cordierite + forsterite + spinel. In runs that used the mixtures as starting materials, two gold capsules were loaded into a single pressure vessel, one with the first mixture, and the other with the second mixture. Each capsule contained 10 to 20 mg of either mixture plus approximately 25 wt.% distilled $H_2O$. The experiments were brought to temperature in about one half hour and stabilized within two hours. Quenching was accomplished by placing the vessel into a cooling jacket and blowing compressed air around the vessel; the temperature dropped to less than 100°C within five minutes. The remaining pressure was released, and the capsules were removed, weighed, punctured, dried, reweighed and then opened for examination. Only runs that showed no weight loss during the experiment were used. Run products were examined optically and by X-ray diffraction, and if complete reaction had not occurred, the direction of reaction was determined by examining X-ray diffractograms and analyzing peak-height ratios. Estimated changes in peak heights of at least 30% for chlorite and lesser but opposite amounts for cordierite, forsterite and spinel were taken as an unequivocal indication of reaction. Experiments that resulted in lesser changes were considered indeterminate. Misinterpretation of reaction direction due to changes in the amount of the possible 7 Å phase was avoided by using the peak-height ratios.

*Phase characterization*

All solid phases were identified by optical properties, morphology, and X-ray powder patterns. Chlorite was characterized by bulk index of refraction and by a unit-cell refinement from powder-diffraction data. Precise characterizations of cordierite, forsterite and spinel were not considered necessary, as their X-ray patterns and optical properties were found to be consistent with published data.

Chlorite was found to occur as fine-grained aggregates of crystals ranging in size from $<1$ to 2 $\mu$m. The bulk index of refraction was bracketed between 1.572 and 1.580 in white light, which compares well with an index of 1.576 listed in Tröger (1979, p. 116–118). The cell parameters were calculated by making four X-ray powder-diffraction scans, two with increasing $2\theta$ and two with decreasing $2\theta$, with silicon metal ($a$ = 5.4305 Å) as an internal standard, Cu$K\alpha$ radiation and a scan rate of ¼°$2\theta$/minute. The means of the peak positions were calculated, and the corresponding $d$-values were processed with the program of Appleman & Evans (1973) to refine the unit-cell parameters. Observed and calculated $d$-values and the refined parameters are presented in Table 1. For comparison, the data from Chernosky (1974) are shown for synthetic clinochlore. Note that the cell dimensions and the volume are smaller than those for clinochlore. Also, the peak intensities of the basal repeats are not equal to each other; the ratios of (001):(002) and (003):(004) were measured to be 0.42 and 0.84. This may indicate the presence of stacking disorder, but was not considered in the following analysis.

The other solid phases were identifiable by their morphology, indices of refraction and X-ray-diffraction patterns. Cordierite occurs as hexagonal prisms as large as 100 $\mu$m in length. Spinel usually occurs as euhedral octahedra less than 1 $\mu$m, although a few grains of up to 2 $\mu$m were noted. Forsterite occurs as anhedral to euhedral grains of platy habit and ranges in size from 1 to 20 $\mu$m. X-ray-diffraction patterns show no evidence of departures from stoichiometry in any of these phases.

TABLE 1. X-RAY POWDER-DIFFRACTION DATA AND REFINED CELL PARAMETERS FOR SYNTHETIC CHLORITES

| h k l | *Synthetic chlorite*[1] $d_{calc}$ | $d_{obs}$ | I(/100)[3] | *Synthetic clinochlore*[2] $d_{obs}$ |
|---|---|---|---|---|
| 0 0 1 | 14.234 | ----- | -- | 14.132 |
| 0 0 2 | 7.117 | ----- | -- | 7.135 |
| 0 0 3 | 4.745 | 4.752 | -- | 4.757 |
| 0 2 0(?) | 4.596 | 4.592 | 40 | ----- |
| 1 1 0 | 4.576 | ----- | -- | 4.588 |
| 1 1 1 | 4.500 | 4.501 | 30 | 4.493 |
| 0 2 1 | 4.374 | 4.384 | 25 | 4.373 |
| 1 1 1 | ----- | ----- | -- | 4.242 |
| 1 1 1(?) | 4.226 | 4.238 | 20 | ----- |
| 1 1 2 | 4.053 | 4.055 | 20 | ----- |
| 0 2 2 | 3.861 | 3.862 | 15 | 3.883 |
| 1 1 2 | 3.674 | ----- | 20 | 3.674 |
| 0 0 4 | 3.558 | 3.560 | -- | 3.572 |
| 0 0 5 | 2.847 | 2.846 | -- | 2.864 |
| 1 1 4 | 2.673 | ----- | -- | 2.691 |
| 2 0 1 | 2.654 | 2.653 | 15 | 2.656 |
| 2 0 2 | 2.580 | 2.579 | 35 | 2.584 |
| 2 0 1 | 2.539 | 2.538 | 100 | 2.540 |
| 2 0 3 | 2.438 | 2.437 | 80 | 2.441 |
| 0 0 6 | 2.380 | 2.376 | 40 | 2.385 |
| 2 0 4 | 2.257 | 2.258 | 35 | 2.260 |
| 2 0 5 | 2.258 | 2.258 | 20 | ----- |
| 0 0 7 | 2.033 | 2.034 | 35 | 2.041 |
| 2 0 4 | 2.004 | 2.004 | 85 | 2.008 |
| 2 0 6 | 1.884 | 1.885 | 35 | 1.889 |
| 2 0 5 | 1.826 | 1.826 | 35 | 1.831 |
| 0 0 8 | 1.779 | 1.781 | 10 | ----- |
| 2 0 7 | 1.717 | ----- | -- | 1.724 |
| 2 0 6 | 1.665 | ----- | 15 | 1.671 |
| 2 0 8 | 1.568 | 1.568 | 55 | 1.573 |
| 0 6 0 | 1.532 | 1.532 | 70 | 1.539 |
| 0 6 2(?) | 1.498 | 1.501 | 20 | 1.502 |
| 0 6 3 | 1.458 | ----- | -- | 1.463 |
| 1 1 9 | 1.448 | ----- | -- | 1.455 |
| 0 0 10 | 1.424 | 1.423 | 20 | ----- |
| 3 3 3 | 1.409 | ----- | -- | 1.412 |
| 2 0 8 | 1.397 | 1.397 | 50 | 1.402 |
| a | 5.317(1) | | | 5.324(1) |
| b | 9.192(2) | | | 9.224(3) |
| c | 14.349(2) | | | 14.420(5) |
| β | 97°8'(1') | | | 97°6'(1') |
| V | 209.515(51) | | | 211.535(84) |

All values of d and cell parameters are given in Å, except volume in cm³/mole.

[1] This study

[2] From Chernosky (1974).

[3] Intensities are given relative to (201). The intensities of the first five orders of the basal repeat are discussed in text.

TABLE 2. EXPERIMENTAL DATA FOR THE EQUILIBRIUM: CHLORITE = CORDIERITE + FORSTERITE + SPINEL + $H_2O$

| Run # | P (bars) | T (°C) | Duration (hrs) | Results[3] |
|---|---|---|---|---|
| Chl-124b[1] | 500(20)[2] | 594(7)[2] | 487 | 80% reaction to Chl (Chl peaks diffuse) |
| Chl-130a,b[1] | 500(25) | 605(5) | 884 | a,b - 80% to Chl |
| Chl-131a,b | 500(25) | 629(5) | 884 | a,b - no apparent reaction |
| Chl-120a,b | 500(25) | 633(6) | 480 | a,b - no apparent reaction |
| Chl-128a,b | 500(20) | 640(5) | 516 | 10% to Cd + Fo + Sp |
| Chl-125b | 1000(25) | 644(5) | 487 | 80% to Chl (Chl peaks diffuse) |
| Chl-129a | 1000(30) | 670(4) | 520 | 30% to Cd + Fo + Sp |
| Chl-112a,b | 1000(20) | 673(5) | 480 | a - 10% to Cd + Fo + Sp; b - 100% to Cd + Fo + Sp |
| Chl-121a,b | 1000(20) | 679(7) | 482 | a - no reaction[4]; b - 100% to Cd + Fo + Sp |
| Chl-113a,b | 1000(50) | 692(5) | 480 | a,b - 100% to Cd + Fo + Sp |
| Chl-101 | 2000(50) | 690(10) | 480 | appearance of Chl[5] |
| Chl-132a,b | 2000(30) | 704(5) | 759 | a - 20% to Cd + Fo + Sp; b - 100% to Cd + Fo + Sp |
| Chl-114a,b | 2000(50) | 705(5) | 480 | a - no reaction[4]; b - 100% to Cd + Fo + Sp |
| Chl-133a,b | 2000(50) | 719(5) | 742 | a,b - 100% reaction to Cd + Fo + Sp |
| Chl-115a,b | 2000(50) | 729(5) | 480 | a,b - 100% reaction to Cd + Fo + Sp |

[1] a represents 4:1 mixture (by weight) of reactants and products, b represents 4:1 mixture of products and reactants.

[2] Numbers in brackets represent errors in the last significant digit(s) of the quoted values.

[3] xx% represents the estimated percentage change in ratios of reactants to products.

[4] The starting material was 100% chlorite.

[5] The starting material was Cd + Fo + Sp.

## *Experimental results*

Reversals of the equilibrium, 20 chlorite [$Mg_{4.75}Al_{2.5}Si_{2.75}O_{10}(OH)_8$] = 4 cordierite + 35 forsterite + 17 spinel + 80 $H_2O$ were made at pressures of 0.5, 1.0 and 2.0 kilobars. The conditions and results of the experiments are listed in Table 2. The amounts of reaction were estimated by averaging the changes in peak-height ratios between chlorite and each of the other solid phases. The results confirm those of Chernosky (1974); he measured the same equilibrium using a chlorite of clinochlore composition. Although the reversals at 0.5 and 1.0 kbar are more constraining than the data of Chernosky, there is no significant displacement of the equilibrium.

The chlorite composition in this study was monitored by checking the position of the (004) peak. No shifts were found between starting materials and run products. The variable water content of cordierite was not measured because the quench rates were not fast enough to prevent rehydration (the pressures and temperatures of the experiments were outside the "quenchable" region of Medenbach *et al.* 1980). The degrees of disorder in spinel and cordierite were not measured.

## THERMODYNAMIC ANALYSIS

A thermodynamic analysis of the experimental data was used to test for internal consistency of the data and to calculate the thermochemical properties of magnesian chlorite, with the data from this and related studies. The free energies of the phases considered were calculated with the equations of state, reference-state properties and heat capacity and volume coefficients from Berman (1988). Aluminum substitution in orthopyroxene and disorder in spinel were calculated as in Berman (1988), and the non-stoichiometric behavior of cordierite was accounted for as outlined below.

## *A model for the composition of cordierite*

Calculation of the free energy of cordierite is complicated by the disorder of aluminum and silicon on the tetrahedral sites and a variable $H_2O$ content. The contribution of disorder on the tetrahedral sites to the free energy was estimated by adding 8 J/mol to the reference-state third-law entropy (Berman 1988). There are several models that predict the $H_2O$ content of cordierite as a function of pressure and temperature (Newton & Wood 1979, Lonker 1981, Martignole & Sisi 1981), but none of them adequately reproduces the available experimental data. As part of this study, a new model was developed that provides a better fit to the experimental data.

### *Crystal chemistry*

The crystal chemistry of cordierite has received considerable attention (Wallace & Wenk 1980, Hochella *et al.* 1979, Cohen *et al.* 1977, Meagher & Gibbs 1977, Gibbs 1966), and will not be considered in detail here. Briefly, cordierite ($Mg_2Al_4Si_5O_{18}\cdot nH_2O$) is a framework silicate made of six-membered rings of Si–O and Al–O tetrahedra stacked along the *z* axis. The rings are connected by three tetrahedra that form channels that allow constituents to pass through the structure. In the channels and between the rings are cavities where ions and molecules may reside. Schreyer (1985) has given an excellent review of cordierite chemistry, especially fluid contents. For the purposes of this study, $H_2O$ is the only channel-site species considered.

In order to develop a reasonable model to describe the $H_2O$ content of cordierite, it is necessary to know how $H_2O$ occurs in the mineral. The occurrence, position and orientation of $H_2O$ in cordierite have been studied by a number of different authors and methods: Aines & Rossman (1984): high-temperature infrared absorption spectroscopy, Carson *et al.* (1982): nuclear magnetic resonance, Armbruster & Bloss (1981): infrared absorption spectroscopy, Hochella *et al.* (1979): high-temperature single-crystal X-ray diffraction, Goldman & Rossman (1977): infrared absorption spectroscopy, Cohen *et al.* (1977): X-ray and neutron diffraction, and Tsang & Ghose (1972): nuclear magnetic resonance. All evidence indicates that $H_2O$ occurs as molecular $H_2O$ and is positioned in the channel cavities; however, it is likely that there is more than

one position in the structure. Natural and synthetic samples of cordierite have been found to have more than one mole of $H_2O$ per unit formula (Leake 1960, Mirwald *et al.* 1979); if the only position is at the center of the channel cavities (0,0,1/4), then the water content would be limited to one mole per unit formula. There is a possibility of $H_4O_4$ substituting for $SiO_4$, but Cohen *et al.* (1977) found no evidence for such substitution. The orientation of water has been examined in many of the above studies. Most authors have concluded that $H_2O$ exists in two orientations: Type I, in which the H–H vector is parallel to the $z$ crystallographic axis, and Type II, in which the H–H vector is perpendicular to $z$ (notation of Wood & Nassau 1967). In both types, the H–O–H plane is in the $y$–$z$ crystallographic plane. There are some suggestions that the $H_2O$ molecule occurs in other orientations. Hochella *et al.* (1979) found, using neutron-density maps, that $H_2O$ exists in only one orientation, and that Type I and II orientations are vector components of that orientation. Cohen *et al.* (1977) also calculated neutron-density maps, but interpreted the results to represent a space average of four orientations. High-temperature infrared absorption spectroscopy at one atmosphere by Aines & Rossman (1984) shows that below 200°C the $H_2O$ is structurally bound, but that at 400°C, $H_2O$ begins to exhibit gas-like characteristics. The spectra obtained indicate that both types of $H_2O$ exist to temperatures of 600°C.

### *Thermodynamic model for cordierite*

Several models for calculating the $H_2O$ content of cordierite have been proposed. Newton & Wood (1979) and Lonker (1981) presented models that are based on the assumption of ideal mixing of anhydrous and hydrous end-members; Newton & Wood chose 1.2 moles of $H_2O$ for the hydrous end-member, and Lonker chose 1.0. In addition, both models incorporated the assumption that the volumes of the two end-members are equal. Newton & Wood fitted the model parameters to the experimental data of Mirwald & Schreyer (1977). Lonker calibrated two models: one to lower-pressure, cold-seal data, and one to higher-pressure, piston-cylinder data. Neither model is consistent with all of the experimental data, and he did not choose between the models. Martignole & Sisi (1981) presented another model in which the behavior of corderite was compared to that of zeolites. However, many of the data they used to calibrate their model are from Schreyer & Yoder (1964), and many of the higher-temperature data are suspect because they lie outside the "quenchable region" shown by Medenbach *et al.* (1980).

An ideal, site-mixing model similar to those of Newton & Wood (1979) and Lonker (1981) was chosen to describe the composition of magnesian cordierite because the existing data are not precise enough to warrant a more complex model. The hydrous end-member was chosen to have 2.0 moles of $H_2O$, because water contents of up to 1.3 moles per unit formula for synthetic cordierite (Mirwald *et al.* 1979) and up to 1.6 moles for natural cordierite (Leake 1960) have been reported. The following equilibrium was used to describe $H_2O$ contents in cordierite:

$$Mg_2Al_4Si_5O_{18} + 2\ H_2O = Mg_2Al_4Si_5O_{18} \cdot 2H_2O \quad (1)$$

The change in free energy for this equilibrium can be expressed as

$$\Delta G_r(P,T) = \Delta G_r^0(P,T) + RT\ln K \quad (2)$$

where $\Delta G_r^0(P,T)$ is the standard-state change in free energy of the reaction, and $K$ is the equilibrium constant for equation (1). If ideal site-mixing in a binary system and a pure vapor phase are assumed, then,

$$RT\ln K = 2RT\ln\left(\frac{x_{hcrd}^{cord}}{1-x_{hcrd}^{cord}}\right) \quad (3)$$

where $x_{hcrd}^{cord}$ refers to the mole fraction of the hydrous cordierite end-member in cordierite.

The free energy of $H_2O$ was calculated using the Haar *et al.* (1984) equation of state, and the heat capacity of anhydrous cordierite was taken from Berman & Brown (1985). The heat capacity of hydrous cordierite was estimated using the predictive model of Berman & Brown (1985) and adding the heat capacity of $H_2O$ to that of anhydrous cordierite. Volumes of the cordierite end-members were assumed to be independent of pressure and temperature. Reference-state enthalpy, entropy and volume of reaction were then fitted to the existing experimental data.

### *Experimental data for $H_2O$ in cordierite*

There are many experimental data available that give the water content of Mg-cordierite as a function of pressure and temperature (Gunter 1977, Duncan 1982, Mirwald *et al.* 1979, Mirwald & Schreyer 1977, Holdaway 1976, Newton 1972, Schreyer & Yoder 1964). The data chosen to calibrate the model here are from Mirwald *et al.* (1979) and Duncan (1982). The other data were not used because of uncertainties in either the experimental or analytical techniques used in those studies. Problems with the experimental and analytical techniques, such as rehydration on quench and analytical uncertainty, are discussed in some detail by Lonker (1981).

Phase-equilibrium data may be expressed as inequalities; the free energy of reaction is greater than zero when the reactants are stable and less than zero when the products are stable. The experimental data of Duncan (1982) are reversed and can easily be cast as such inequalities; adjustments to the quoted pressures, temperatures and compositions were made using assumed errors of ±20 bars, ±10°C and ±10%. The data of Mirwald *et al.* (1979) are given as "equilibrium" compositions, although inherently they represent bracketing compositions. In order to test these data for internal consistency, each point was split arbitrarily into upper and lower brackets. As the data were presented graphically, estimates were made of the pressures and temperatures of the experiments, and errors in pressure and temperature were assumed to be ±3% and ±10°C. Compositions were adjusted using the relative error, quoted as ±6%.

*Results*

The adjusted experimental data were first tested for internal consistency, and then used to calculate internally consistent enthalpies, entropies and volumes for the two end-members, using the technique of mathematical programming (Berman *et al.* 1986). With the assumed model and errors quoted above, we found the data of Mirwald *et al.* (1979) to be internally inconsistent. Expanding the errors in pressure and temperature had only small effects in resolving the inconsistencies; however, by relaxing the errors in composition to ±10% (pressure and temperature errors remaining ±3% and ±10°C), a feasible solution to the set of constraining inequalities was obtained. The larger error in composition is probably justified because the analytical error was quoted as relative error, and the error may have been greater for individual measurements.

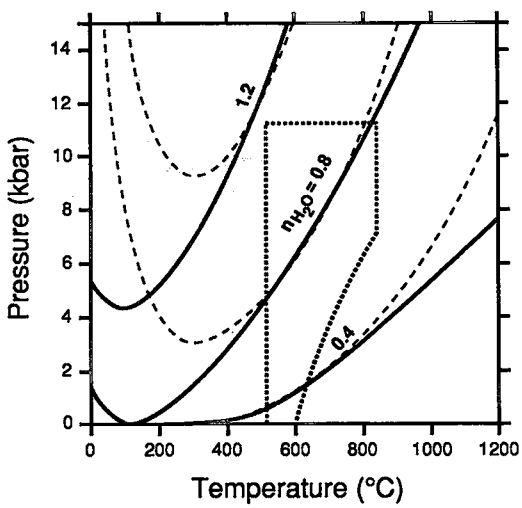


FIG. 1. Isopleths of cordierite; n($H_2O$) represents the number of moles of $H_2O$ per 18-oxygen unit formula. The dashed and bold lines are calculated from properties derived using the heat capacity of "zeolitic water" and steam, respectively, to estimate the heat capacity of hydrous cordierite. The dotted line shows the range of experimental *P–T–X* data used in the analysis.

TABLE 3. DIFFERENCES IN ENTHALPIES, THIRD-LAW ENTROPIES AND VOLUMES FOR ANHYDROUS AND HYDROUS CORDIERITE ENDMEMBERS *

| $\Delta H\ (P_r,T_r)$ (J/mol) | $\Delta S\ (P_r,T_r)$ (J/mol/K) | $\Delta V\ (P_r,T_r)$ ($cm^3$/mol) |
|---|---|---|
| -563493.8 | 156.665 | 23.066 |

* ($Mg_2Al_4Si_5O_{18} \cdot 2H_2O$ – $Mg_2Al_4Si_5O_{18}$)

The heat capacity of the hydrous end-member was estimated in two ways: firstly, by adding the heat capacity of "zeolitic" water from Berman & Brown (1985) to that of anhydrous cordierite, and secondly, by adding the heat capacity of steam. Both models are consistent with the data, but they diverge beyond the pressure and temperature range of the experimental data. Figure 1 shows the calculated isopleths of cordierite using the two models. Note that at low temperatures the isopleths calculated from the models show changes in slope. There is some evidence that this behavior is real and not merely a numerical artifact of the models; Schreyer (1985) showed a diagram in which the same behavior was observed in an experimental study where the $H_2O$ content of cordierite was measured at low temperatures (Jochum *et al.* 1983). At low temperatures, the model using the heat capacity of "zeolitic water" may be more reasonable; however, the estimate of heat capacity using steam is preferred for the following reasons: evidence from the high-temperature infrared absorption study of Aines & Rossman (1984) indicates that $H_2O$ exists in cordierite, at least partly, in a gas-like state at temperatures above 400°C (at one atmosphere); the heat capacity of "zeolitic" water is calculated from calorimetric data for analcime to temperatures of 400°C, whereas the lower limit of the cordierite hydration data is 500°C.

Mirwald (1982) presented evidence of a nonquenchable phase transition in anhydrous cordierite, which may affect the $H_2O$ content of cordierite. Dynamic experiments were conducted in a piston-cylinder apparatus, and discontinuities were found in the piston-pressure *versus* displacement curves, which he interpreted to be the result of a phase transition. He predicted the transition to be at 2.2 kilobars, 25°C and at 8.8 kilobars, 900°C. The effects of the phase transition were tested by including high-pressure polymorphs of anhydrous and hydrous cordierite in the model. Smaller errors in composition of ±8% were sufficient to fit the data successfully

with this model; however, we chose the simpler model because the differences in calculated compositions between the two models were small.

The final stage of modeling consisted of calculating a set of thermochemical properties for reaction (1). The errors used for all the chosen experimental data were ±3%, ±10°C and ±10% in pressure, temperature and composition, and heat-capacity coefficients for hydrous cordierite were estimated using steam. Ranges in internally consistent thermochemical properties were calculated by maximizing or minimizing the values for each property, and the final properties were chosen as the midpoints of those ranges.

The differences in reference-state enthalpies, entropies and volumes for the two end-members are given in Table 3. Isopleths of cordierite calculated from equation (2) with the data in Table 3 are shown in Figure 2. Also shown, for comparison, are isopleths calculated using the model of Newton & Wood (1979). At pressures above 6 kilobars, the models are in fair agreement, but at lower pressures, their model predicts $H_2O$ contents that are approximately half the values predicted with this model (Fig. 2).

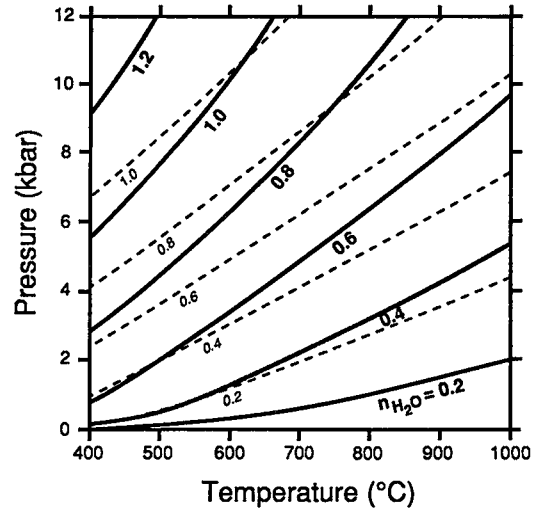


FIG. 2. Water contents of magnesian cordierite in equilibrium with $H_2O$ as a function of pressure and temperature. The isopleths are labeled with the number of moles of $H_2O$ (n) per 18-oxygen unit formula. The bold lines are calculated from the data in Table 3, and the dotted lines are calculated using the model of Newton & Wood (1979).

## A MODEL FOR THE COMPOSITION OF MAGNESIAN CHLORITE

### *Crystal chemistry*

The crystal chemistry of chlorite has been reviewed recently by Bailey (1988) and will not be described in detail here. Briefly, the structure of 14-Å chlorite is made up of alternating 2:1 (talc-like) and interlayer (brucite-like) sheets. The 2:1 sheet is made up of tetrahedra and octahedra and has an ideal composition of $(R^{2+},R^{3+})_3(Si_{4-x}R^{3+}_x)O_{10}(OH)_2$, and the interlayer is made up of octahedra and has the ideal composition $(R^{2+},R^{3+})_3(OH)_6$. The overall formula may be approximated by $(R^{2+}_{6-y-z}R^{3+}_y\square_z)(Si_{4-x}R^{3+}_x)O_{10}(OH)_8$ (Bailey 1980). In the formula unit, there are six octahedrally coordinated sites, three in the interlayer sheet and three in the 2:1 sheet, and four tetrahedrally coordinated sites, all in the 2:1 sheet. The 2:1 sheets have a net negative charge, resulting from the replacement of silicon by aluminum, and the sheets of octahedra have a net positive charge, resulting from the replacement of a divalent ion with a trivalent ion.

The distribution of atoms among the sites in chlorite is not well known. There is some evidence from refinements of single-crystal X-ray and neutron-diffraction data for IIb and Ia chlorites (Rule & Bailey 1987, Bailey 1986, Joswig *et al.* 1980, Phillips *et al.* 1980, Brown & Bailey 1963, Steinfink 1958, 1961), NMR studies (Thompson 1984), calculations of electrostatic energy (Bish & Giese 1981), and compositional and charge-balance constraints (Foster 1962). Nemecz (1981, p. 240) reported that the concentration of aluminum in the tetrahedral sites attains 70% in $T_1$ and 20% in $T_2$. However, Rule & Bailey (1987) summarized existing data and predicted that the tetrahedrally coordinated cations, as well as the octahedrally coordinated cations in the 2:1 layer, are disordered in IIb chlorite in most cases. They also pointed out that existing data suggest that the octahedrally coordinated cations of the interlayer sheets are at least partly ordered, with a trivalent cation in the centrosymmetric site $M(4)$.

There are 12 possible polytypes of the trioctahedral chlorite structure, based on geometrical arguments (Brown & Bailey 1962). However, approximately 80% of natural samples contain the IIb polytype (Brown & Bailey 1962), indicating that it is the most stable of the possible polytypes. Very little stacking disorder was found by Spinnler *et al.* (1984); they used single-crystal X-ray methods, high-resolution transmission electron microscopy and electron diffraction to study the stacking sequence of a natural chlorite close to clinochlore in composition.

### *Thermodynamic model for magnesian chlorite*

Solution properties of magnesian chlorite were modeled using the end-members $Mg_6Si_4O_{10}(OH)_8$ (Chls) and $(Mg_4Al_2)(Al_2Si_2)O_{10}(OH)_8$ (Coph), chosen to span the compositional range of natural

chlorite compiled by Foster (1962): 1.2 to 3.2 Al atoms per 18-oxygen formula unit ($n_{Al}$). Molar volumes of the end members at 298 K and 1 bar were estimated by linear extrapolation from the clinochlore volume of Berman (1988) using the volume data of Jenkins & Chernosky (1986); coefficients for the volume function of Berman (1988) were assumed to be those of clinochlore. The method of Helgeson *et al.* (1978) was used to estimate end-member reference-state entropies and heat-capacity coefficients using clinochlore, periclase and corundum properties from Berman (1988). Thermochemical properties for all other phases are those of Berman (1988).

The enthalpies of the end members were fitted to experimental data for the following equilibria (using enstatite with a 3-oxygen formula):

$$5\ \text{Coph} = \text{Cordierite} + 5\ \text{Forsterite} + 8\ \text{Spinel} + 20\ H_2O \quad (4)$$

$$5\ \text{Chls} + 2\ \text{Cordierite} = 30\ \text{Enstatite} + 4\ \text{Spinel} + 20\ H_2O \quad (5)$$

$$1\ \text{Coph} + 8\ \text{Enstatite} = 1\ \text{Cordierite} + 5\ \text{Forsterite} + 4\ H_2O \quad (6)$$

The technique of mathematical programming (Berman *et al.* 1986) was used to calculate the thermochemical properties of the chlorite end-members from the experimental data of this study and of Chernosky (1974) for reaction (4), and the data of Jenkins & Chernosky (1986) for reactions (5) and (6). Other experimental data used by Berman (1988) to derive the properties of clinochlore were not included here because of uncertainty in the composition of the chlorite in the experiments. Jenkins & Chernosky observed that the chlorite in their experiments became more aluminous than clinochlore ($n_{Al}=2.0$) at temperatures above 600°C, and reached $n_{Al}=2.4$ at chlorite breakdown. Consequently, the modeling was carried out with the composition of chlorite constrained to be between 2.0 and 2.4 $n_{Al}$ for the data of Jenkins & Chernosky (1986) and between 2.4 and 2.5 $n_{Al}$ for the data of this study.

Ideal mixing of aluminum in chlorite was modeled in the following manner. The six octahedral sites of the chlorite structure were divided into two groups, denoted as four *M*1 and two *M*2 sites, and the four tetrahedral sites were divided into two *T*1 and two *T*2 sites. The following equations were used to calculate the activities of the end-members:

$$a^{\text{Chl}}_{\text{Chls}} = (x^{M1}_{\text{Mg}})^4 (x^{M2}_{\text{Mg}})^2 \quad (7)$$

$$a^{\text{Chl}}_{\text{Coph}} = (x^{M1}_{\text{Mg}})^4 (x^{M2}_{\text{Al}})^2 \quad (8)$$

where $a^{\text{Chl}}_{\text{Coph}}$ and $a^{\text{Chl}}_{\text{Chls}}$ are the activity of Coph and Chls in chlorite, respectively, $x^{M1}_{\text{Mg}}$ is the atomic fraction of magnesium on *M*1 (assumed equal to one), $x^{M2}_{\text{Al}}(n_{Al}/4)$ is the atomic fraction of aluminum on *M*2, and $x^{M2}_{\text{Mg}}$ $[n_{Mg}-4)/2]$ is the atomic fraction of Mg on *M*2 (n is the number of atoms of Al or Mg per formula unit). This model incorporates the assumptions that aluminum mixes on only two of the six octahedral sites and that there is coupled substitution of aluminum on the tetrahedral site. These assumptions were considered appropriate because, on the basis of crystal-chemical evidence, it is not likely that mixing occurs on all of the octahedral sites; it seems most reasonable to assume that, owing to charge-balance constraints, there is coupled substitution of aluminum on the tetrahedral site.

Analysis of the experimental data led to enthalpies of formation (298 K, 1 bar) for the Al-free end member (Chls) of approximately $-8760 \pm 5$ kJ/mole. This enthalpy was considered to be unreasonable because the Al-free chlorite would be more stable than chrysotile (the low-temperature phase with the same formula), with a corresponding enthalpy of −8726 kJ/mole. Several other activity models were tested in an attempt to decrease the calculated stability of Chls, and the results showed that the fitted enthalpy was not sensitive enough to different models based on ideal mixing. The maximum contribution from ideal mixing was calculated by assuming mixing on all of the octahedral sites and all of the tetrahedral sites (no coupled substitution); however, this made a difference in the calculated enthalpy of Chls of only about +5 kJ/mole. Therefore, the Al-free chlorite end-member was constrained to be less stable than chrysotile at 25°C and 1 bar, and a symmetrical, non-ideal excess free-energy term was fitted to the experimental data (using the original activity models).

TABLE 4. THERMODYNAMIC PROPERTIES OF MAGNESIAN CHLORITE END-MEMBERS

| | $\Delta H_f$ (298,1)[1] (J/mol) | S (298,1)[2] (J/mol/K) | V (298,1)[3] (J/bar) |
|---|---|---|---|
| Chls | -8720000.00 | 445.0 | 21.377 |
| Coph | -9014400.16 | 425.0 | 20.917 |

Heat capacity coefficients for the function,

$$C_p = k_0 + k_1 T^{-0.5} + k_2 T^{-2} + k_3 T^{-3}$$

| | $k_0$ | $k_1$ | $k_2$ | $k_3$ |
|---|---|---|---|---|
| Chls | 1225.8 | -11589 | 1590803 | -1386186496 |
| Coph | 1202.7 | -10845 | -1590803 | -1126319872 |

Volume function coefficients for the function,

$$\frac{V^{T,P}}{V^{298,1}} = 1 + v_1(P-P_r) + v_3(T-T_r)$$

| | $v_1$ ($10^6$) | $v_3$ ($10^8$) |
|---|---|---|
| Chls | -0.18195 | 2.64515 |
| Coph | -0.18195 | 2.64515 |

Chls is the aluminum-free chlorite endmember ($Mg_6Si_4O_{10}(OH)_8$).
Coph is the aluminous chlorite endmember ($Mg_4Al_4Si_2O_{10}(OH)_8$).

[1] Enthalpy of formation from the elements at 298 K and 1 bar.
[2] Third-Law entropy at 298 K and 1 bar.
[3] Volume at 298 K and 1 bar.

## Results

The final fitted properties of the two chlorite endmembers are listed in Table 4. They reproduce all the experimental data within their uncertainties, using the activity model above and an excess free-energy parameter of -121.2 kJ/mole. These properties were used to calculate stable mineral assemblages and chlorite composition using the program THERIAK (DeCapitani & Brown 1987); thermodynamic data for all other phases were taken from Berman (1988). The composition of cordierite was calculated with the model presented above, and that of orthopyroxene was approximated using a site-mixing model between the enstatite and magnesium-Tschermaks end members. All other phases were considered to be stoichiometric. Comparisons between calculated equilibria and constraining experimental data are shown in Figures 3 and 4, where the calculated breakdown composition of chlorite is shown as $n_{Al}$. Figures 5 and 6 show comparisons between the experimental data of Jenkins & Chernosky (1986) and the predicted temperature-dependence of chlorite composition at 3 and 14 kbars. The model results predict the same trends seen in the experimental data, and there is good agreement at temperatures near the breakdown of chlorite. At 3 kbars the calculated compositions agree well with the experimentally determined values for starting compositions of 2.4 and 2.8 $n_{Al}$, and there is fair agreement for a starting composition of clinochlore (2.0 $n_{Al}$). At 14 kbars and lower temperatures, the experimentally determined compositions are slightly more aluminous than clinochlore, the predicted composition. However, the experiments were mainly synthesis experiments, and the chlorite compositions may not represent equilibrium.

## Discussion

Magnesian chlorite occurs in a number of different metamorphic rocks, such as metamorphosed ultramafic rocks, metadolomites, high-pressure metapelitic rocks and corundum-bearing metamorphic rocks. Of course, there are many occurrences of chlorite in metamorphosed pelitic rocks; however, the solution properties of iron-magnesium chlorite are not well known, and we will not discuss them in this paper. The aluminum content of magnesian chlorite depends on pressure, temperature and bulk composition, and the calculations summarized below explore quantitatively the effect that these variables have on chlorite composition. The results identify those assemblages in which the composition of chlorite should be useful as a petrogenetic indicator and also indicate which assemblages warrant attention in future field and experimental studies.

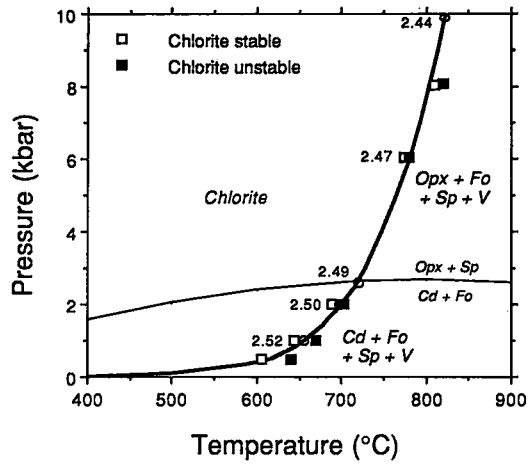


FIG. 3. High-temperature stability of magnesian chlorite from 1 bar to 10 kbars, calculated from the data in Table 4. Open squares represent constraining experiment reversals in which chlorite is stable with respect to forsterite + spinel + cordierite or orthopyroxene. Filled squares represent experimental reversals where chlorite is unstable. The constraining data from this study are plotted for the low-pressure reaction chlorite = cordierite + forsterite + spinel + $H_2O$; other data at higher pressure are from Jenkins & Chernosky (1986). All experiments are plotted with nominal pressures and temperatures; no adjustments were made for errors. Numbers beside circles on the *PT* curves give the calculated breakdown composition of chlorite in terms of aluminum atoms per 18-oxygen unit formula ($n_{Al}$).

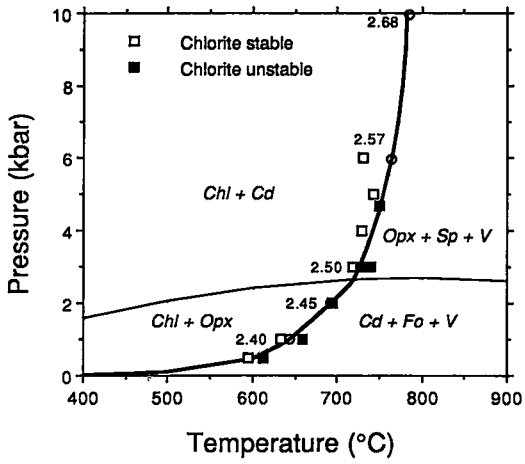


FIG. 4. Stability of magnesian chlorite + cordierite or orthopyroxene from 1 bar to 10 kbars. These two equilibria complete the invariant point of Figure 3. Symbols and abbreviations as in Figure 3. Plotted experimental data are from Jenkins & Chernosky (1986).

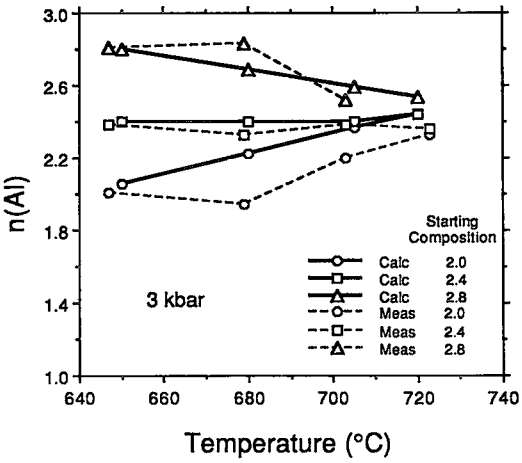


FIG. 5. Comparison of predicted *versus* measured chlorite compositions at 3 kbars. Solid lines connect calculated compositions, and dashed lines connect measured compositions (Jenkins & Chernosky 1986). Starting compositions are the initial composition ($n_{Al}$) of chlorite for both calculated points and measured data. $n_{Al}$ is the number of aluminum atoms per 18-oxygen formula unit of chlorite.

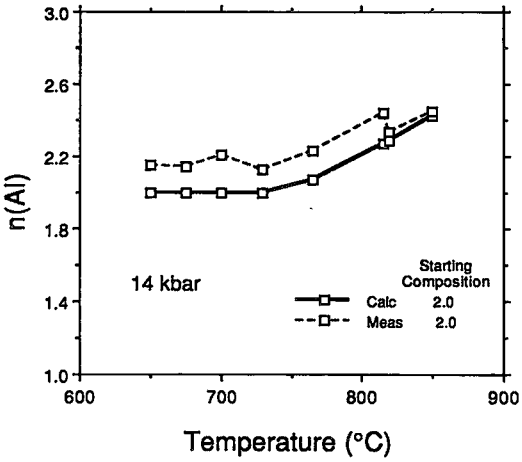


FIG. 6. Comparison of predicted *versus* measured chlorite compositions (Jenkins & Chernosky 1986) at 14 kbars. Lines, data and $n_{Al}$ as in Figure 5.

An example of stable assemblages and chlorite composition is shown in Figure 7, calculated for 600°C and 3 kbars in the chemical system MgO–$Al_2O_3$–$SiO_2$–$H_2O$. Note that in the model system, the aluminum content of chlorite is fixed for a given pressure and temperature, when it is in equilibrium with two other solid phases. Four bulk compositions (points A–D on Fig. 7) were chosen to give three-phase mineral assemblages representative of the above rock-types, and to show how predicted composition of chlorite changes with pressure and temperature for low-, intermediate-, and high-aluminum assemblages. Details of the calculations for each bulk composition are discussed separately below, and comparisons are made with data from natural assemblages. Equilibration temperatures and pressures for each of the natural assemblages were taken from the estimates of the original work if available, or else from phase relations calculated with the GEO–CALC program (Brown *et al.* 1988), using ideal site-mixing to account for Fe–Mg mixing in the minerals.

*Bulk composition A*

Chlorite is buffered to its lowest aluminum content in assemblages found in metamorphosed ultramafic rocks. Bulk composition A (Fig. 7) results in such assemblages. The predicted stable assemblages are chlorite + forsterite plus, with increasing temperature, antigorite, talc, anthophyllite, and enstatite. In all cases, the composition of the chlorite is predicted to become more aluminous with increasing temperature and less aluminous with increasing pressure (Fig. 8).

The four predicted phase-assemblages are observed in metamorphosed ultramafic rocks, although chlorite compositional data were located only for the three highest-temperature assemblages. Frost (1975) reported the composition of chlorite coexisting with forsterite – talc, forsterite – anthophyllite and forsterite – orthopyroxene (points b, c and d on Fig. 8) from the Paddy-Go-Easy Pass area of Washington. Using his estimate for $P(H_2O)$ of 2 to 3 kbars, the upper-temperature limit of the forsterite – talc assemblage is approximately 650–660°C, the forsterite – anthophyllite assemblage is stable between 650° and 700°C, and the forsterite – orthopyroxene assemblage is stable with chlorite from 700°C to chlorite breakdown at about 720°C (assuming pure $H_2O$ in the vapor phase). The plotted data show wider ranges in temperature, reflecting the effects of possible reduction in the activity of water [estimated $a(H_2O)$ between 0.7 and 1.0]. Both Trommsdorff & Evans (1969) and Arai (1975) reported the composition of chlorite coexisting with olivine and orthopyroxene. Trommsdorff & Evans estimated conditions of equilibration of about 600°C and 4 kbars for their samples from the Lepontine Alps (point a on Fig. 8), indicative of low activity of $H_2O$ stabilizing orthopyroxene relative to amphibole or talc. Arai estimated metamorphic conditions of 700°C and 2.5 kbars (point e on Fig. 8). The predicted increase in the aluminum content of chlorite is well documented in the natural chlorite, although the model predictions are shifted to a slightly higher content of aluminum.

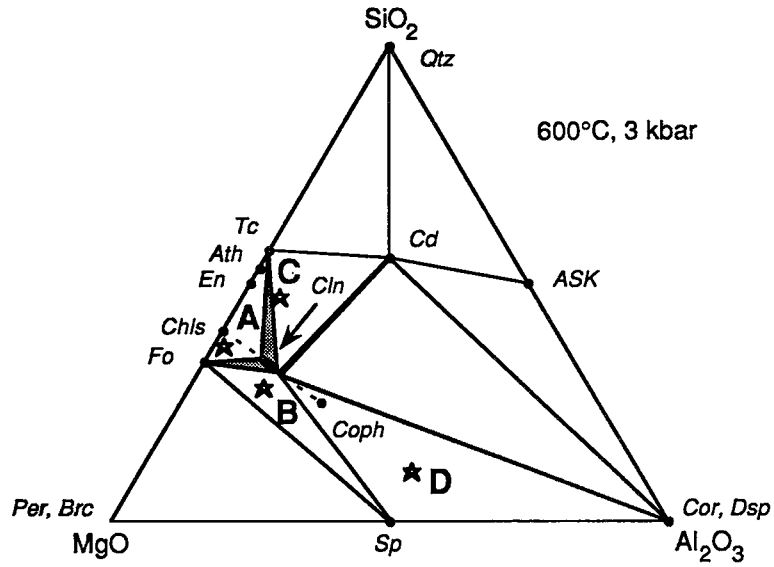


FIG. 7. Chemographic diagram of stable assemblages, projected from pure $H_2O$ and calculated for 600°C and 3 kbars. Stars labeled A–D represent the bulk compositions that are discussed in the text. Shaded areas are two-phase fields; there are also small two-phase fields of cordierite – chlorite and corundum – chlorite. Abbreviations Ath anthophyllite, ASK aluminosilicate, Brc brucite, Cd cordierite, Chls Al-free chlorite end-member, Cln clinochlore, Coph Al-chlorite end-member, Cor corundum, Dsp diaspore, En enstatite, Fo forsterite, Per periclase, Qtz quartz, Sp spinel, Tc talc.

*Bulk compositions B and C*

Magnesian chlorite is buffered to an intermediate-aluminum content in assemblages found in metamorphosed dolomites, peridotites and high-pressure pelitic rocks. Bulk composition B (Fig. 7) results in an assemblage representative of the first two rock types, and C (Fig. 7) results in an assemblage representative of the last. Two assemblages are predicted for bulk composition B: chlorite – brucite – spinel and, at higher temperature, chlorite – forsterite – spinel. Because no data were found for the lower-temperature assemblage, only the behavior of the higher-temperature assemblage is shown in Figure 9. In contrast to the results summarized above for bulk composition A, the model predicts only a slight variation in chlorite composition with increasing pressure and temperature. The assemblage chlorite – talc – quartz is predicted for bulk composition C, and its high-temperature stability is limited by the breakdown of chlorite + quartz (520°C, 1 kbar; 660°C, 8 kbars). In contrast to the results from the other intermediate-aluminum assemblage (chlorite – forsterite – spinel), chlorite composition becomes more aluminous with increasing temperature and less aluminous with increasing pressure (Fig. 10).

The compositions of natural chlorite reported for the chlorite – forsterite – spinel assemblage are scattered, and there are no apparent trends with temperature or pressure. The predicted composition of chlorite agrees well with two chlorite compositions reported by Lieberman & Rice (1986), point b on Figure 9, as part of their study of the Seiad ultramafic complex in California. The samples were taken from chloritic blackwall rocks and marbles, where the estimated metamorphic conditions were 760–800°C and 7–8 kbars. The agreement between predicted values and those reported in other studies is less promising. The rock types and the estimated pressures and temperatures are: Frost (1975), metaperidotite, 3 kbars, 670–720°C; Bucher-Nurminen (1981), metadolomite, 7.5 kbars, 760–800°C; Arai (1975), metamorphosed ultramafic rocks, 2.5 kbars, 670–720°C; Bucher-Nurminen (1982), metadolomite, 5 kbars, 605–690°C; Rice (1977), metacarbonates, 1 kbar, 495-630°C. For these examples, the predicted composition of chlorite is more aluminous than the measured composition; whereas there may be uncertainty in the pressure and temperature estimates of the field studies, discrepancies would remain because the predicted compositions are not sensitive to pressure and temperature. Further study is necessary to resolve the differences

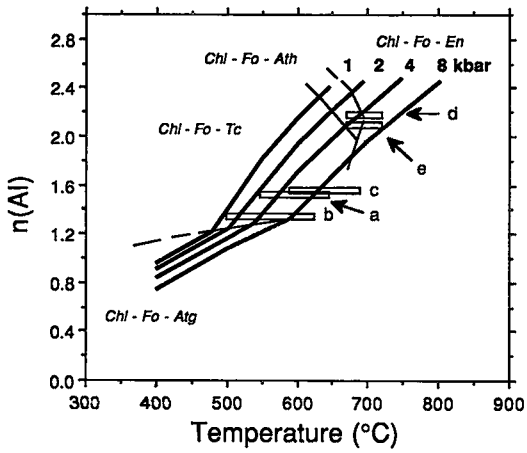


FIG. 8. Predicted composition of magnesian chlorite for low-aluminum bulk composition A (see Fig. 7). Thick lines are isobars labeled from 1 to 8 kbars. Stable mineral assemblages are separated by the fine lines; boxes a – e show the compositions of natural chlorite at estimated pressures and temperatures. Box a: Trommsdorff & Evans (1969), chlorite – forsterite – enstatite, 4 kbars. Box b: Frost (1975), chlorite – forsterite – talc, 3 kbars. Box c: Frost (1975), chlorite – forsterite – anthophyllite, 3 kbars. Box d: Frost (1975), chlorite – forsterite – enstatite, 3 kbars. Box e: Arai (1975), chlorite – forsterite – enstatite, 2.5 kbars. Atg antigorite, Chl chlorite, all other abbreviations defined in Figure 7.

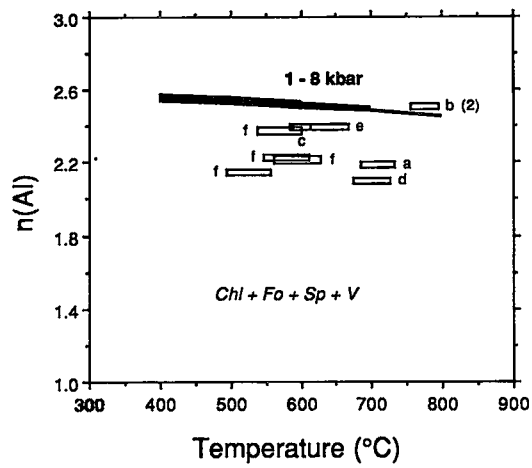


FIG. 9. Predicted composition of magnesian chlorite for intermediate-aluminum bulk composition B (see Fig. 7). Lines are isobars labeled from 1 to 8 kbars, and boxes a –f show the compositions of natural chlorite at estimated pressures and temperatures. Box a: Frost (1975), 3 kbars. Boxes b: Lieberman & Rice (1986), 7.5 kbars. Box c: Bucher-Nurminen (1981), 4 kbars. Box d: Arai (1975), 2.5 kbars. Box e: Bucher-Nurminen (1982), 5 kbars. Boxes f: Rice (1977), 1 kbar. Abbreviations as in previous figures. The assemblage chlorite – forsterite spinel is metastable with respect to chlorite – brucite – spinel at temperatures below approximately 530°C at 1 kbar and 630°C at 8 kbars.

between measured and predicted compositions.

The assemblage chlorite – talc – quartz has been identified in pelitic rocks that have been metamorphosed under whiteschist-facies conditions (high pressure and low temperature), and it is stable up to the breakdown of chlorite + quartz. Chopin (1981) reported compositions of chlorite from chlorite – talc – quartz – phengite assemblages found in the Western Alps, where the estimated pressure and temperature were 4–6 kbars and 450–490°C. This assemblage has been reported also by Abraham & Schreyer (1976), in their study of a piemontite schist from Serbia, Yugoslavia. Rough estimates of 9–12 kbars and 450–640°C were made for the ranges of metamorphic pressure and temperature, using the stabilities of the assemblages talc – muscovite and chlorite – quartz for the low- and high-temperature limits (*cf.* Fig. 6 in Abraham & Schreyer). The model predicts values that are in reasonable agreement with the measured values (Fig. 10).

*Bulk Composition D*

Chlorite is buffered to its highest aluminum content in rocks containing corundum. The predicted assemblages for bulk composition D (Fig. 7) are, with

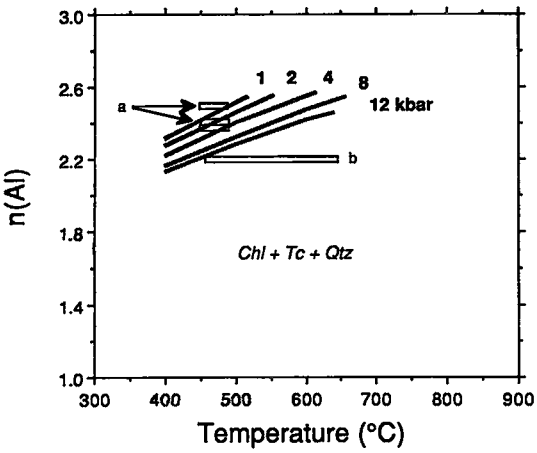


FIG. 10. Predicted composition of magnesian chlorite for intermediate-aluminum bulk composition C (see Fig. 7). Lines are isobars labeled 1 to 12 kbars; boxes a and b show compositions of natural chlorite at estimated pressures and temperatures. Boxes a: Chopin (1981), 4–6 kbars. Box b: Abraham & Schreyer (1976), 9–12 kbars. Abbreviations as in previous figures.

increasing temperature, chlorite – diaspore – spinel, chlorite – corundum – spinel, and chlorite – spinel – cordierite or enstatite. The lower-temperature assemblage is stable up to 400°C at 3 kbars, 480°C at 8 kbars, and is not considered here. The assemblage chlorite – corundum – spinel is limited at higher temperatures by the stability of chlorite + corundum (see Fig. 11). The predicted composition of chlorite becomes less aluminous with increasing temperature and decreasing temperature (Fig. 11). This behavior is opposite to that predicted for ultramafic assemblages. Two other chlorite-bearing assemblages are predicted to be stable in aluminous bulk compositions: chlorite – corundum – aluminosilicate – $H_2O$ and chlorite – corundum – cordierite – $H_2O$. The predicted compositions (2.6–2.8 $n_{Al}$) show little dependence on pressure and temperature.

Chlorite composition from corundum-bearing rocks has been reported by Oliver & Jones (1965) and Schreyer *et al.* (1981). Oliver & Jones reported the composition of a chlorite coexisting with corundum and sapphirine and estimated metamorphic pressures and temperatures of 1.4 kbars and 500–700°C. The predicted composition of chlorite (using the assemblage chlorite – corundum –spinel) is similar to that measured by Oliver & Jones (Fig. 11). A more direct comparison could not be made because the thermodynamic properties of sapphirine are not well known. Schreyer *et al.* reported the composition of a chlorite ($n_{Al}$ = 2.48) coexisting with corundum – andalusite – fuchsite, and estimated metamorphic pressures and temperatures of 2–3 kbars and 400–500°C. Using the estimated pressures and temperatures, the calculated $n_{Al}$ for chlorite in equilibrium with corundum and andalusite varies from 2.81 to 2.96. This range in aluminum content is higher than the measured value; the probable explanation for the higher predicted Al-contents is that the natural chlorite is chromium-rich (0.26 atoms per formula unit).

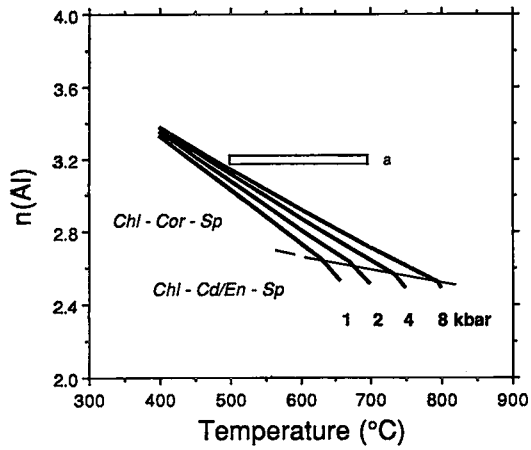


FIG. 11. Predicted composition of magnesian chlorite for high-aluminum bulk composition D (see Fig. 7). Thick lines are isobars labeled from 1 to 8 kbars, the fine line separates the stable mineral assemblages, and box a shows a composition of a chlorite coexisting with sapphirine + corundum: Oliver & Jones (1969), 1.4 kbars. Abbreviations as in previous figures.

## CONCLUSIONS

The experimental data gathered for this study confirm the data of Chernosky (1974) for the breakdown of magnesian chlorite to cordierite + forsterite + spinel + $H_2O$. They also show that this particular equilibrium is not sensitive to the aluminum content of chlorite. However, the data from this study, combined with experimental data from other studies, provide loose constraints on the solution properties of the magnesium-Tschermaks exchange in magnesian chlorite. A thermodynamic model that includes both ideal and nonideal mixing has been fitted to the experimental data, where the stability of the low-temperature phase *chrysotile* was used as an additional constraint on the free energy of an Al-free chlorite end-member.

The model for the Al-content in magnesian chlorite derived above has been used to predict chlorite composition for stable mineral assemblages as a function of pressure and temperature. Several assemblages have been identified in which chlorite composition should be useful as a petrogenetic indicator. For assemblages typical of metamorphosed ultramafic rocks (chlorite – forsterite – orthopyroxene and chlorite – forsterite – talc), chlorite composition is predicted to be sensitive to temperature and pressure (0.5 $n_{Al}$ per 100°C and 0.1–0.2 $n_{Al}$ per 1 kbar). Chlorite becomes more aluminous with increasing temperature and decreasing pressure, a result in agreement with the composition of natural chlorite. Chlorite composition is also predicted to be sensitive to temperature in aluminous, corundum-bearing assemblages, but in contrast to the ultramafic compositions, chlorite becomes less aluminous with increasing temperature (0.3 $n_{Al}$ per 100°C). Assemblages that buffer the aluminum content of chlorite to intermediate values are found in metadolomites and in pelitic rocks that have been metamorphosed at high pressure and low temperature. The composition of chlorite predicted for the high-pressure metapelite assemblage, chlorite – talc – quartz, becomes more aluminous with increasing temperature and less aluminous with increasing pressure, in agreement with data from natural chlorite. For the assemblage chlorite – forsterite – spinel, common in impure marbles and also found in metamor-

phosed ultramafic rocks, chlorite composition is predicted to be insensitive to pressure and temperature; however, comparison with natural chlorite shows a need for further study.

There are still not enough experimental data to fully constrain the properties of the magnesium-Tschermaks exchange in magnesian chlorite. However, the results of this study suggest several mineral assemblages that would be useful for constraining chlorite composition in future experimental studies: chlorite – forsterite – talc or orthopyroxene, chlorite – forsterite – spinel, chlorite – talc – quartz, and chlorite – corundum – spinel. A more reliable model for the thermodynamic properties of magnesian chlorite would help in understanding the geological environments in which such chlorite is present, and provide a more solid foundation for the study of the more complicated Fe–Mg chlorite.

## Acknowledgements

We thank Tom Brown, "Capi" DeCapitani, Paul Bartholomew and Lyle Hammerstrom for their help and constructive advice at various stages of this study. We also thank Drs. B.R. Frost and J.V. Chernosky for thorough reviews that helped improve the manuscript; of course they are not responsible for any mistakes or omissions that may remain. NSERC is gratefully acknowledged for funding through grant 67–4222 to H.J. Greenwood and OGP0037234 to R.G. Berman.

## References

Abraham, K. & Schreyer, W. (1976): A talc–phengite assemblage in piemontite schist from Brezovica, Serbia, Yugoslavia. *J. Petrol.* **17**, 421-439.

Aines, R.D. & Rossman, G.R. (1984): The high temperature behavior of water and carbon dioxide in cordierite and beryl. *Am. Mineral.* **69**, 319-327.

Appleman, D.E. & Evans, H.T., Jr. (1973): Job 9214: indexing and least-squares refinement of powder diffraction data. *U. S. Geol. Surv., Comput. Contrib.* **20** (NTIS Doc. **PB2-16188).**

Arai, S. (1975): Contact metamorphosed dunite–harzburgite complex in the Chugoku District, western Japan. *Contrib. Mineral. Petrol.* **52**, 1-16.

Armbruster, T. & Bloss, F.D. (1981): Mg-cordierite: Si/Al ordering, optical properties, and distortion. *Contrib. Mineral. Petrol.* **77**, 332-336.

Bailey, S.W. (1980): Structures of layer silicates. *In* Crystal Structures of Clay Minerals and their X-ray Identification (G.W. Brindley & G. Brown, eds.). *Mineral. Soc., Monogr.* **5**, 1-124.

_____ (1986): Re-evaluation of ordering and local charge-balance in Ia chlorite. *Can. Mineral.* **24**, 649-654.

_____ (1988): Chlorites: structures and crystal chemistry. *In* Hydrous Phyllosilicates (Exclusive of Micas) (S.W. Bailey, ed.). *Rev. Mineral.* **19**, 347-403.

Berman, R.G. (1988): Internally-consistent thermodynamic data for minerals in the system $Na_2O$–$K_2O$–CaO–MgO–FeO–$Fe_2O_3$–$Al_2O_3$–$SiO_2$–$TiO_2$–$H_2O$–$CO_2$. *J. Petrol.* **29**, 445-522.

_____ & Brown, T.H. (1985): Heat capacity of minerals in the system $Na_2O$–$K_2O$–CaO–MgO–FeO–$Fe_2O_3$–$Al_2O_3$–$TiO_2$–$SiO_2$–$H_2O$–$CO_2$: representation, estimation and high temperature extrapolation. *Contrib. Mineral. Petrol.* **89**, 168-183.

_____, Engi, M., Greenwood, H.J. & Brown, T.H. (1986): Derivation of internally-consistent thermodynamic data by the technique of mathematical programming: a review with application to the system MgO–$SiO_2$–$H_2O$. *J. Petrol.* **27**, 1331-1364.

Bish, D.L. & Giese, R.F., Jr. (1981): Interlayer bonding in IIb chlorite. *Am. Mineral.* **66**, 1216-1220.

Brown, B.E. & Bailey, S.W. (1962): Chlorite polytypism. I. Regular and semi-random one-layer structures. *Am. Mineral.* **47**, 819-850.

_____ & _____ (1963): Chlorite polytypism. II. Crystal structure of a one-layer Cr–chlorite. *Am. Mineral.* **48**, 42-61.

Brown, T.H., Berman, R.G. & Perkins, E.H. (1988): GE0-CALC: software package for calculation and display of pressure–temperature–composition phase diagrams using an IBM or compatible personal computer. *Comput. Geosci.* **14**, 279-290.

Bucher-Nurminen, K. (1981): Petrology of chlorite–spinel marbles from NW Spitsbergen (Svalbard). *Lithos* **14**, 203-213.

_____ (1982): Mechanism of mineral reactions inferred from textures of impure dolomitic marbles from East Greenland. *J. Petrol.* **23**, 325-343.

Carson, D.G., Rossman, G.R. & Vaughan, R.W. (1982): Orientation and motion of water molecules in cordierite: a proton nuclear magnetic resonance study. *Phys. Chem. Miner.* **8**, 14-19.

Chernosky, J.V., Jr. (1974): The upper stability of clinochlore at low pressure and the free energy of formation of Mg-cordierite. *Am. Mineral.* **59**, 496-507.

_____, Berman, R.G. & Bryndzia, L.T. (1988): Stability, phase relations, and thermodynamic properties of chlorite and serpentine group minerals. *In* Hydrous Phyllosilicates (Exclusive of Micas) (S.W. Bailey, ed.). *Rev. Mineral.* **19**, 295-346.

CHOPIN, C. (1981): Talc–phengite: a widespread assemblage in high-grade pelitic blueschists of the Western Alps. J. Petrol. **22**, 628-650.

COHEN, J.P., ROSS, F.K. & GIBBS, G.V. (1977): An X-ray and neutron diffraction study of hydrous low cordierite. *Am. Mineral.* **62**, 67-78.

DECAPITANI, C. & BROWN, T.H. (1987): The computation of chemical equilibrium in complex systems containing non-ideal solutions. *Geochim. Cosmochim. Acta* **51**, 2639-2652.

DUNCAN, I.J. (1982): *The Evolution of the Thor–Odin Gneiss Dome and Related Geochronological Studies.* Ph.D. thesis, Univ. British Columbia, Vancouver, British Columbia.

FOSTER, M.D. (1962): Interpretation of the composition and a classification of the chlorites. *U.S. Geol. Surv., Prof. Pap.* **414-A.**

FROST, B.R. (1975): Contact metamorphism of serpentinite, chloritic blackwall and rodingite at Paddy-Go-Easy Pass, central Cascades, Washington. *J. Petrol.* **16**, 272-313.

GIBBS, G.V. (1966): The polymorphism of cordierite. I. The crystal structure of low cordierite. *Am. Mineral.* **51**, 1068-1087.

GOLDMAN, D.S. & ROSSMAN, G.R. (1977): Channel constituents in cordierite. *Am. Mineral.* **62**, 1144-1157.

GUNTER, A.E. (1977): *An Experimental Study of Synthetic Cordierites.* Ph.D. thesis, Carleton Univ., Ottawa, Ontario.

HAAR, L., GALLAGHER, J. & KELL, G.S. (1984): *NBS/NRC Steam Tables. Thermodynamic and Transport Properties and Computer Programs for Vapor and Liquid States of Water in SI Units.* McGraw Hill, New York.

HELGESON, H.C., DELANY, J.M., NESBITT, H.W. & BIRD, D.K. (1978): Summary and critique of the thermodynamic properties of rock-forming minerals. *Am. J. Sci.* **278-A.**

HOCHELLA, M.F., JR., BROWN, G.E., JR., ROSS, F.K. & GIBBS, G.V. (1979): High-temperature crystal chemistry of hydrous Mg- and Fe-cordierites. *Am. Mineral.* **64**, 337-351.

HOLDAWAY, M.J. (1976): Mutual compatibility relations of the $Fe^{2+}$–Mg–Al silicates at 800°C and 3 kb. *Am. J. Sci.* **276**, 285-308.

JENKINS, D.M. & CHERNOSKY, J.V., JR. (1986): Phase equilibria and crystallochemical properties of Mg-chlorite. *Am. Mineral.* **71**, 924-936.

JOCHUM, C., MIRWALD, P.W., MARESCH, W. & SCHREYER, W. (1983): The kinetics of $H_2O$ exchange between cordierite and fluid during retrogression. *Fortschr. Mineral.* **61**, 103-105.

JOSWIG, W., FUESS, H., ROTHBAUER, R., TAKÉUCHI, Y. & MASON, S.A. (1980): A neutron diffraction study of a one-layer triclinic chlorite (penninite). *Am. Mineral.* **65**, 349-352.

KITTRICK, J.A. (1982): Solubility of two high-Mg and two high-Fe chlorites using multiple equilibria. *Clays Clay Miner.* **30**, 167-179.

LAIRD, J. (1988): Chlorites: metamorphic petrology. *In* Hydrous Phyllosilicates (Exclusive of Micas) (S.W. Bailey, ed.). *Rev. Mineral.* **19**, 405-453.

LEAKE, B.E. (1960): Compilation of chemical analyses and physical constants of natural cordierites. *Am. Mineral.* **45**, 282-298.

LIEBERMAN, J.E. & RICE, J.M. (1986): Petrology of marble and peridotite in the Seiad ultramafic complex, northern California, USA. *J. Metamorph. Geol.* **4**, 179-199.

LONKER, S.W. (1981): The P–T–X relations of the cordierite – garnet – sillimanite – quartz equilibrium. *Am. J. Sci.* **281**, 1056-1090.

MARTIGNOLE, J. & SISI, J.-C. (1981): Cordierite–garnet–$H_2O$ equilibrium: a geological thermometer, barometer and water fugacity indicator. *Contrib. Mineral. Petrol.* **77**, 38-46.

MEAGHER, E.P. & GIBBS, G.V. (1977): The polymorphism of cordierite. II. The crystal structure of indialite. *Can. Mineral.* **15**, 43-49.

MEDENBACH, O., MARESCH, W.V., MIRWALD, P.W. & SCHREYER, W. (1980): Variation of refractive index of synthetic Mg-cordierite with $H_2O$ content. *Am. Mineral.* **65**, 367-373.

MIRWALD, P.W. (1982): A high-pressure phase transition in cordierite. *Am. Mineral.* **67**, 277-283.

_____, MARESCH, W.V. & SCHREYER, W. (1979): Der Wassergehalt von Mg–Cordierit zwischen 500° und 800°C sowie 0,5 und 11 kbar. *Fortschr. Mineral.* **57**, 101-102.

_____ & SCHREYER, W. (1977): Die stabile und metastabile Abbaureaktion von Mg-Cordierit in Talk, Disthen und Quarz und ihre abhängigkeit vom Gleichgewichtswassergehalt des Cordierits. *Fortschr. Mineral.* **55**, 95-97.

NEMECZ, E. (1981): *Clay Minerals.* Akadémiai Kiadó, Budapest, Hungary (English translation).

NEWTON, R.C. (1972): An experimental determination of the high-pressure stability limits of magnesian cordierite under wet and dry conditions. *J. Geol.* **80**, 398-420.

_____ & WOOD, B.J. (1979): Thermodynamics of water in cordierite and some petrologic consequences of cordierite as hydrous phase. *Contrib. Mineral. Petrol.* **68,** 391-405.

OLIVER, R.L. & JONES, J.B. (1965): A chlorite-corundum rock from Mount Painter, South Australia. *Mineral. Mag.* **35,** 140-145.

PHILLIPS, T.L., LOVELESS, J.K. & BAILEY, S.W. (1980): $Cr^{3+}$ coordination in chlorites: a structural study of ten chromian chlorites. *Am. Mineral.* **65,** 112-122.

RICE, J.M. (1977) Contact metamorphism of impure dolomitic limestone in the Boulder aureole, Montana. *Contrib. Mineral. Petrol.* **59,** 237-259.

RULE, A.C. & BAILEY, S.W. (1987): Refinement of the crystal structure of a monoclinic ferroan clinochlore. *Clays Clay Miner.* **35,** 129-138.

SCHREYER, W. (1985): Experimental studies on cation substitutions and fluid incorporation in cordierite. *Bull. Minéral.* **108,** 273-291.

_____, WERDING, G. & ABRAHAM, K. (1981): Corundum-fuchsite rocks in greenstone belts of southern Africa: petrology, geochemistry, and possible origin. *J. Petrol.* **22,** 191-231.

_____ & YODER, H.S., JR. (1964): The system Mg-cordierite - $H_2O$ and related rocks. *Neues Jahrb. Mineral., Abh.* **101,** 271-342.

SPINNLER, G.E., SELF, P.G., IIJIMA, S. & BUSECK, P.R. (1984): Stacking disorder in clinochlore chlorite. *Am. Mineral.* **69,** 252-263.

STEINFINK, H. (1958): The crystal structure of chlorite. I. A monoclinic polymorph. *Acta Crystallogr.* **11,** 191-195.

_____ (1961): Accuracy in structure analysis of layer silicates: some further comments on the structure of prochlorite. *Acta Crystallogr.* **14,** 198-199.

STOESSELL, R.K. (1984): Regular solution site-mixing model for chlorites. *Clays Clay Miner.* **32,** 205-212.

TERRY, R.D. & CHILINGAR, G.V. (1955): Summary of: "Concerning some additional aids in studying sedimentary formations". *J. Sediment. Petrol.* **25,** 229-234.

THOMPSON, J.G. (1984): $^{29}Si$ and $^{27}Al$ nuclear magnetic resonance spectroscopy of 2:1 clay minerals. *Clay Miner.* **19,** 229-236.

TRÖGER, W.E. (1979): *Optical Determination of Rock-Forming Minerals. I. Determinative Tables.* E. Schweizerbart'sche Verlagsbuchhandlung (Nägele u. Obermiller), Stuttgart, Germany.

TROMMSDORFF, V. & EVANS, B.W. (1969): The stable association enstatite - forsterite - chlorite in amphibolite facies ultramafics of the Lepontine Alps. *Schweiz. Mineral. Petrogr. Mitt.* **49,** 325-332.

TSANG, T. & GHOSE, S. (1972): Nuclear magnetic resonance of $^{1}H$ and $^{27}Al$ and Al-Si order in low cordierite, $Mg_2Al_4Si_5O_{18}{\cdot}nH_2O$. *J. Chem. Phys.* **56,** 3329-3332.

WALLACE, J.H. & WENK, H.-R. (1980): Structure variation in low cordierites. *Am. Mineral.* **65,** 96-111.

WALSHE, J.L. (1986): A six-component chlorite solid solution model and the conditions of chlorite formation in hydrothermal and geothermal systems. *Econ. Geol.* **81,** 681-703.

_____ & SOLOMON, M. (1981): An investigation into the environment of formation of the volcanic-hosted Mt. Lyell copper deposits using geology, mineralogy, stable isotopes, and a six-component chlorite solid solution model. *Econ. Geol.* **76,** 246-284.

WOOD, D.L. & NASSAU, K. (1967): Infrared spectra of foreign molecules in beryl. *J. Chem. Phys.* **47,** 2220-2228.

YODER, H.S., Jr. (1952): The $MgO-Al_2O_3-SiO_2-H_2O$ system and the related metamorphic facies. *Am. J. Sci., Bowen Vol.,* 569-627.

*Received September 15, 1989, revised manuscript accepted April 27, 1990.*